

# Reproducibility of diurnal variation of summertime precipitation by a nonhydrostatic model

Masaomi Nakamura\*, Teruyuki Kato and Syugo Hayashi

\*Meteorological Research Institute, Tsukuba, Ibaraki, 305-0052, JAPAN

manakamu@mri-jma.go.jp

## 1. Introduction

The Kanto District, located in central Japan, consists of the Kanto Plain and mountainous areas in the north and west and it faces the Pacific Ocean in the south and east. Due to its geographical features, convective precipitation associated with thermally-induced circulation are frequently observed in the afternoon and evening in summer. Many authors investigated the characteristic of these convective activities from observational point of view. On the other hand, studies from reproducibility or forecasting aspects by using numerical models are very limited.

Summertime convective precipitation is one of important targets of forecast in the Kanto District and to evaluate the performance of numerical model and to clarify the problem in reproducing it, if exists, is an interesting work still left. In this study, we evaluate the reproducibility of observational characteristics in the diurnal variation of summertime precipitation around the Kanto District, based on one-month simulation results by the Japan Meteorological Agency (JMA) NonHydrostatic Model (hereafter referred to as NHM).

## 2. Experimental design

First, NHM was run at 5-km grid spacing from 03 to 21 JST (Japan Standard Time), with initial and boundary conditions given from JMA operational mesoscale analysis of 3-hourly intervals. Then, NHM was run at 1-km grid spacing from 04 to 21JST with initial and boundary conditions given from the NHM5km results. The experiments were carried out for one month of August 2010.

The specifications of NHM5km and 1km are nearly the same. Both models use Mellor-Yamada level-3 scheme improved by Nakanishi and Niino and cloud microphysics predicting both the mixing ratio and number density of water cloud, ice cloud, rain, snow and graupel. Both models have horizontal grid numbers of 500 and 400 in the x and y directions, respectively, and stretched 50 vertical layers with a depth of 40m near the surface and about 900m at the model top (~22km). A big difference between the two models is in that NHM5km uses the Kain-Fritsch cumulus convection scheme, while NHM1km does not. Details of NHM are described in Saito et al. (2007) and literatures cited there.

## 3. Results

Figure 1 shows the horizontal distribution of the frequency of precipitation (hereinafter abbreviated as FP) from observation and NHM1km. The observation data, JMA radar-rain gauge analyzed precipitation (referred to as AP) which originally has an horizontal resolution of 1km, and NHM1km results are used after being spatially averaged over 5km-square grid. FP is obtained by counting the number of hourly precipitation exceeding 1mm at each 5km-grid point during a 3-hour period, 15-16, 16-17 and 17-18JST for each day and then averaging over the month. The figure indicates that the model fails to reproduce an increase of FP over the northern mountain area in the late afternoon.

FP of NHM1km increases from 12JST to 15JST, following that of observation (AP), but stops increasing

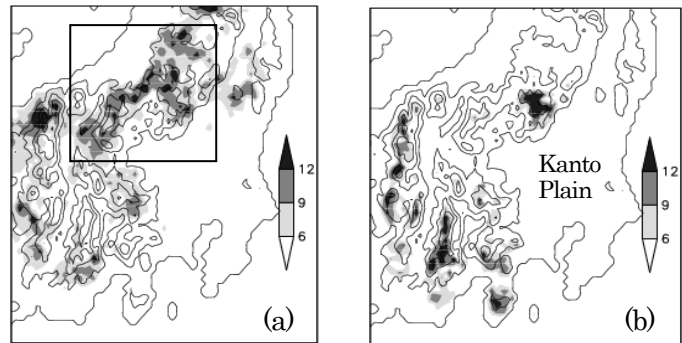


Figure 1. Observed (a) and NHM1km's (b) monthly mean frequency of hourly-precipitation exceeding 1mm on the 5-km grid. Contours are drawn at 500m intervals. The whole domain, including the Kanto District, is that of NHM1km.

afterwards (Fig.2a). The diurnal increase of precipitable water (dPW) of the model is not enough (fig.2b); dPW is defined as an increment of PW from a value at 06JST, nearly when PW has a minimum value. The negative bias of dPW increases toward peak time of around 18JST. The scatter diagram for the region including the northern mountain area (Fig.3) indicates that, irrespective of geographical location, plain or mountain, model's PW has a negative bias.

Figure 4 shows that the horizontal distribution of the bias of model-predicted PW at 18JST; model's PW is corrected for the difference between model topography and GPS station heights by a rate 1.5mm/100m (roughly estimated from Fig.3). Positive-bias points are seen only over southern coastal areas. The model has a negative bias in other area. Considering the fact that a diurnal increase of PW is mainly caused by transport of water vapor from low altitude areas to mountains and to upper layers there, Figures 2b and 3 suggest that there is a possibility that the model does not have sufficient ability to transport water vapor to higher-altitude layers.

If we draw figures similar to Fig.3 and 4 for initial hours, it is seen that model's PW is insufficient even for these hours, though less in amount compared to later hours. The insufficient initial PW could affect the following time evolution of the model.

#### 4. Summary and concluding remarks

- 1) NHM fails to reproduce summertime precipitation peak in the late afternoon, especially over the northern mountain area in the Kanto District.
- 2) The model also underestimates PW over the area, compared with GPS observation. PW of the model is an underestimate, even in initial hours.
- 3) This bias in the initial field could affect the time evolution of model fields and cause insufficient peaks in FP and PW in the model, but an possibility that they are caused by some defects in the model could not be denied.
- 4) The result of NMM5km is not described here, but it shows essentially the same features as NHM1km.

It is left for future study to identify factors causing NHM's FP and PW errors and improve its reproducibility for summer-time convective precipitation.

#### 5. References

Saito, K., J. Ishida, K. Aranami, T. Hara, T. Segawa, M. Narita, and Y. Honda, 2007: Nonhydrostatic atmospheric models and operational development at JMA. *J. Meteor. Soc. Japan*, **85**, 271-304.

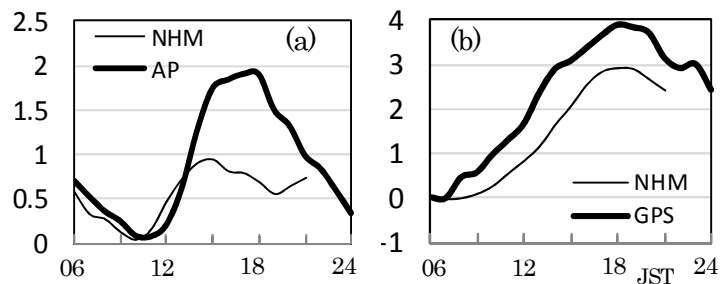


Figure 2. (a) Diurnal variation of monthly-mean frequency of hourly-precipitation exceeding 1mm, averaged over the 5km land grids within the rectangular region in Fig.1a. Thick and thin solid lines represent observation and NHM1km results, respectively. (b) Same as (a) but for monthly mean dPW (mm) averaged over GPS points.

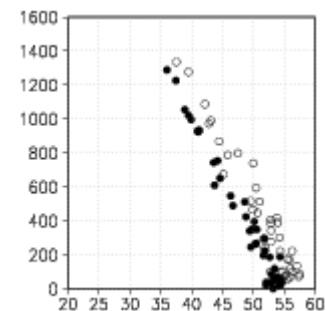


Figure 3. Scatter diagram for monthly mean PW (mm) and station height (m) for GPS (open circle) within the rectangular region in Fig.1a and for NHM1km (filled circle) at 18JST.

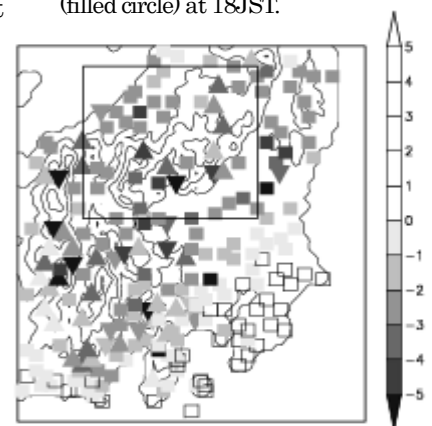


Figure 4. Monthly mean NHM1km-minus-GPS PW at 18JST.  $\Delta$ ( $\nabla$ ) represents a point where the model topography is higher (lower) than GPS-station height by more than 100m.  $\square$  otherwise. Positive values are white colored.